Covariant Theory of the Disintegration of the Deuteron by Pions and Photons at High Energy*

D. J. George†
Institute of Theoretical Physics, Department of Physics, Stanford University, Stanford, California
(Received 11 September 1967)

A covariant form of the Austern model of the disintegration of the deuteron is developed within the framework of relativistic perturbation theory. It is shown that the model reproduces the recent polarization and asymmetry measurements, but suffers from the same defects as the noncovariant calculations.

1. INTRODUCTION

When the first cross-section results for photodisintegration at high energy became available, an enhancement at about 300-MeV laboratory energy was seen. It was natural to associate this with the enhancement seen in the πN system which is now called the $\Delta(1236)$. Austern[1] and Wilson[2] suggested a definite model for the effect. They considered that the enhancement was because of the process shown in Fig. 1.

Their cross-section estimates were in reasonable agreement with experiment except that the peak occurred at slightly too high an energy and the differential cross section was too large in the forward and in the backward directions. A few years ago, Gourdin and Salin[3] calculated the cross sections for photoproduction off nucleons and elastic πN scattering using the isobar method. This treats the resonance as an elementary particle with a complex mass. They obtained excellent agreement with experiment. No attempts at a formulation of the photodisintegration using their method was attempted at that time, probably because of the very complicated γ algebra involved. The reason such a calculation is now possible is that computer programs which can perform γ algebra are now available.[4]

Liu[5,6] has measured the asymmetry and the polarization in photodisintegration. In the case of the asymmetry he obtained rather bad disagreement with the existing theory of Partovi.[7] Liu mentioned in his paper[5] that he believed meson effects to be the cause of this disagreement. Indeed, we think we can explain his results with the present model.

When the theory of the photodisintegration had been formulated, we found that we had two parameters which had to be fixed by experiment. The photodisintegration data has an unusual amount of spread and so we decided to calculate pionic disintegration and use that data to fix our parameters. Then armed with the values from pionic disintegration we could judge between the rival sets of data on photodisintegration.

The diagrams (Figs. 2–4) which we use to describe the disintegration processes are simply those which are valid in the low and intermediate energy range as discussed by Le Bellac *et al.*[8] and Vasavada,[9] together with the resonance diagram corresponding to the Austern model. No other graphs are known to play any significant part at these energies.

2. METHOD AND NOTATION

The method we shall employ is relativistic perturbation theory. The justification for this is the belief in nearest singularity dominance. Many authors have used this so-called isobar method and we can feel fairly confident of the results.

A. Kinematics

The metric, γ-matrix convention, and similar things are treated in Appendix A. The 4-momenta of the external particles are labelled by Fig. 5. They are, in the center-of-mass (c.m.) system,

$$\begin{aligned} d&=(d^0;-\mathbf{k}), & p_1&=(E;\mathbf{p}),\\ k&=(k^0;\mathbf{k}), & p_2&=(E;-\mathbf{p}). \end{aligned} \tag{1}$$

The Mandelstam variables are

$$\begin{aligned} s&=(k+d)^2=(p_1+p_2)^2=4E^2,\\ t&=(k-p_1)^2=(d-p_2)^2=M^2+m^2-2(d^0E-\mathbf{p}\cdot\mathbf{k}),\\ u&=(k-p_2)^2=(d-p_1)^2=M^2+m^2-2(d^0E+\mathbf{p}\cdot\mathbf{k}). \end{aligned} \tag{2}$$

We shall also use

$$\begin{aligned} w&=\mathbf{p}\cdot\mathbf{k}/m^2,\\ y&=p^2/m^2,\\ z&=\cos\theta,\\ \sigma&=\mu^2/m^2,\\ \eta&=m^*/m. \end{aligned} \tag{3}$$

An important scale factor is α, where $\alpha^2=MB$ and B is the binding energy of the deuteron. In the definitions

* Research sponsored by the Air Force Office of Scientific Research, Office of Aerospace Research, U. S. Air Force, under AFOSR Contract No. AF49(638)-1389.

† Present address: Department of Physics, Purdue University, Lafayette, Ind.

[1] N. Austern, Phys. Rev. **100**, 1522 (1955).
[2] R. R. Wilson, Phys. Rev. **104**, 218 (1956).
[3] M. Gourdin and Ph. Salin, Nuovo Cimento **27**, 193 (1963).
[4] A. C. Hearn, Commun. Am. Comp. Machy. **9**, 573 (1966).
[5] F. F. Liu, Phys. Letters **11**, 306 (1964); Phys. Rev. **138**, B1443 (1965).
[6] F. F. Liu, D. Lundquist, and B. H. Wiik, in Proceedings of the International Conference on Low Intermediate Energy Electromagnetic Interaction, Dubna (USSR), 1967 (unpublished).
[7] F. Partovi, Ann. Phys. (N. Y.) **27**, 79 (1964).
[8] M. Le Bellac, F. M. Renard, and J. Tran Thanh Van, Nuovo Cimento **33**, 594 (1964); **34**, 450 (1964).
[9] K. V. Vasavada, Ann. Phys. (N. Y.) **35**, 191 (1965).

of the invariant amplitudes we shall use

$$Q=\tfrac{1}{2}(p_1+p_2),$$
$$q=\tfrac{1}{2}(p_1-p_2). \tag{4}$$

B. Invariant Amplitudes

In the usual way, the T matrix is defined by

$$S_{fi}=\delta_{fi}+[i/(2\pi)^2][m/(4k^0d^0E^2)^{1/2}]\times\delta^{(4)}(k+d-p_1-p_2)T_{fi}. \tag{5}$$

Then the T matrix can be expanded:

$$T_{fi}=\bar{u}(p_1)\sum_i H_i(s,t,u)I_iC\bar{u}^T(p_2), \tag{6}$$

where C is the charge-conjugation matrix which has the value $\gamma_0\gamma_2$, H_i are the invariant coefficients, and I_i the invariant amplitudes.

The invariant amplitudes for photodisintegration are taken from Le Bellac *et al.* and given in Table I(a) for reference. The invariant amplitudes for the pionic disintegration of the deuteron in Table I(b) are slightly different from those chosen by Vasavada. They have greater similarity to those of photodisintegration and also seem to give simpler coefficients. Also in Table I we give the symmetry of the I_i under the interchange of p_1 and p_2. Denoting such an interchange by a prime, we find

$$I_i=\epsilon_i I_i'. \tag{7}$$

C. Helicity Amplitudes

In Appendix B we show how the helicity amplitudes $F_{i\pm}$ are defined and how they can be calculated from the invariant coefficients.

The asymmetry $\Sigma(\theta)$ is defined as

$$\Sigma(\theta)\equiv[d\sigma/d\Omega|_\perp-d\sigma/d\Omega|_\parallel]/[d\sigma/d\Omega|_\perp+d\sigma/d\Omega|_\parallel], \tag{8}$$

where the subscripts $\perp$ and $\parallel$ refer to photons polarized perpendicular and parallel to the production plane. In terms of the helicity amplitudes it can be shown that

$$\Sigma(\theta)=-2\,\mathrm{Re}[F_{1+}F_{3-}^*+F_{1-}F_{3+}^*-F_{2+}F_{2-}^*-F_{4+}F_{6-}^*-F_{4-}F_{6+}^*+F_{5+}F_{5-}^*]/\sum|F_{i\epsilon}|^2. \tag{9}$$

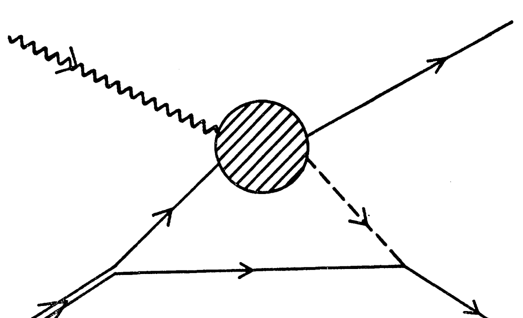

FIG. 1. The Austern model. In this diagram, as in Figs. 2–5, the solid lines represent nucleons, the double lines represent deuterons, the wavy lines represent photons *or* pions, and the broken lines represent pions. The shaded area here represents the resonant process.

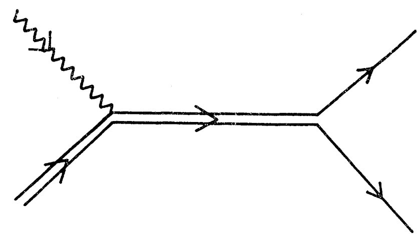

FIG. 2. The deuteron-pole diagram. As explained in the text, this diagram only appears in photodisintegration.

The polarization $P(\theta)$ of the proton in the final state is defined as

$$P(\theta)\equiv[d\sigma/d\Omega|_\uparrow-d\sigma/d\Omega|_\downarrow]/[d\sigma/d\Omega|_\uparrow+d\sigma/d\Omega|_\downarrow], \tag{10}$$

where the subscripts $\uparrow$ and $\downarrow$ denote protons polarized up or down with respect to the production plane. It is then easy to show that

$$P(\theta)=2\,\mathrm{Im}[F_{1+}F_{4+}^*+F_{1-}F_{4-}^*+F_{2+}F_{5+}^*+F_{2-}F_{5-}^*+F_{3+}F_{6+}^*+F_{3-}F_{6-}^*]/\sum|F_{i\epsilon}|^2 \tag{11}$$

for photodisintegration, and that

$$P(\theta)=2\,\mathrm{Im}[F_{1+}F_{2+}^*+F_{1-}F_{2-}^*+F_{3+}F_{3-}^*]/\sum|F_{i\epsilon}|^2 \tag{12}$$

for pionic disintegration. Finally, the cross section is

$$\frac{d\sigma}{d\Omega}=\frac{m^2}{(8\pi E)^2}\frac{p}{k}\frac{2}{J}\sum_{i=1}^{2J}\sum_{\epsilon=\pm}|F_{i\epsilon}|^2, \tag{13}$$

where J, the spin multiplicity of the initial state, has the value 6 for photodisintegration and 3 for pionic disintegration.

3. VERTICES AND PROPAGATORS

A. dNN Vertex

This has been treated extensively in the literature[10] and we shall just quote the results. For a deuteron of polarization vector U decaying into two nucleons with

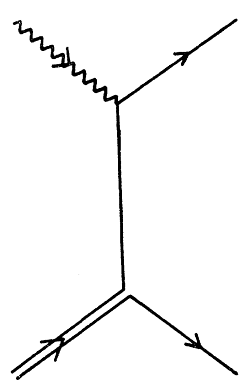

FIG. 3. The nucleon-pole diagram.

[10] R. Blankenbecler and L. F. Cook, Phys. Rev. **119**, 1745 (1960); J. Tran Thanh Van, Nuovo Cimento **30**, 1100 (1963); M. Gourdin, M. Le Bellac, F. M. Renard, and J. Tran Thanh Van, *ibid.* **37**, 524 (1965); I. J. McGee, Phys. Rev. **158**, 1500 (1967).

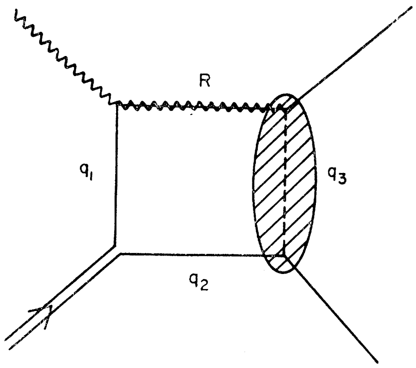

FIG. 4. The resonant diagram. In this case, the combination solid/wavy line represents the $\Delta(1236)$. The shaded area represents the Selleri-Ferrari pion factor.

relative momentum q we have

$$\Gamma_{dNN}=F(aU-bU\cdot q)w(q^2)\,, \tag{14}$$

where F is a coupling constant and has the value $(8\pi/m)^{1/2}N$, where $N^2=155.8\pm5.7$ MeV; $w(q^2)$ is a form factor

$$w(q^2)=(\beta^2-\alpha^2)/(\beta^2+q^2)\,,\quad \beta=5.18\alpha\,; \tag{15}$$

a and b are two constants

$$a=1+\rho/\sqrt{2}\,,\quad mb=3m^2\rho/\sqrt{2}\alpha^2+\tfrac{1}{2}a\,, \tag{16}$$

where ρ is the D-state mixing parameter. From static properties of the deuteron ρ is inferred to be about 3%.

This vertex function (14) is not exact. The approximations implied by such a vertex are discussed in Ref. 10.

B. Nucleon and Deuteron Vertices

There are two types of $NN\gamma$ vertices. The Dirac coupling is

$$H_{\text{int}}=e(\bar{\psi}\gamma\cdot\epsilon\psi+\text{H.c.})\,, \tag{17}$$

where H.c. means Hermitian conjugate. The Pauli coupling is

$$H_{\text{int}}=(e\kappa/2m)(\bar{\psi}k\gamma\cdot\epsilon\psi+\text{H.c.})\,, \tag{18}$$

where κ, the anomalous magnetic moment has the values $\kappa_p=1.793$ for the proton and $\kappa_n=-1.913$ for the neutron.

The well-known $NN\pi$ vertex is

$$H_{\text{int}}=g(\bar{\psi}\gamma_5\psi+\text{H.c.})\,, \tag{19}$$

with $g^2/4\pi=14.5$.

Sakita and Goebel[11] showed the $dd\gamma$ vertex to be given by

$$\langle U'd'|H_{\text{int}}|\epsilon k;Ud\rangle=-e[U'\cdot U\epsilon\cdot(d+d') -2\mu_d(\epsilon\cdot Uk\cdot U'-\epsilon\cdot U'k\cdot U)]\,, \tag{20}$$

with $\mu_d=0.8576$. Quadrupole-type terms have been omitted as they are very small (see, for example, Ref. 8).

[11] B. Sakita and C. Goebel, Phys. Rev. **127**, 1787 (1962).

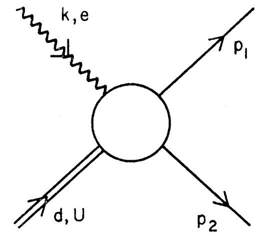

FIG. 5. The general-reaction diagram.

C. Δ Vertices and Propagators

Gourdin and Salin[3] showed that the dominant $\Delta N\pi$ and $\Delta N\gamma$ couplings are

$$H_{\text{int}}=(\lambda/\mu)(\bar{\psi}_\mu\psi\partial^\mu\phi_\pi+\text{H.c.})\,, \tag{21}$$

$$H_{\text{int}}=-(eC_3/\mu)(\bar{\psi}\gamma_\mu\gamma_5\psi_\nu+\text{H.c.})f^{\mu\nu}\,. \tag{22}$$

They gave $\lambda=2.07$ and $C_3=0.37$, but a reanalysis of the data by Dalitz and Sutherland[12] indicates $\lambda=2.16$ and $C_3=0.29$, and these are the values which we use.

The one-pion-exchange picture of $\Delta N\to NN$ must be modified by the Ferrari-Selleri[13] form factor

$$F(t)=A-B\mu^2/(t-C\mu^2)\,, \tag{23}$$

where $A=0.28$, $B=3.42$, and $C=5.75$. This was included to estimate effects of final-state interactions. It does not significantly affect the results of the calculation.

The Δ propagator is still in dispute. We shall use the one proposed by Mohan and Agarwal[14] which is the most direct generalization of the nonrelativistic spin-$\frac{3}{2}$ projection operator. It is

$$P_{\mu\nu}(R)/(R^2-m^{*2}),\quad P_{\mu\nu}(R)=[-\tfrac{2}{3}(g_{\mu\nu}-R_\mu R_\nu/m^{*2}) +(i/3m^*)\epsilon_{\mu\nu\lambda\sigma}\gamma_5\gamma^\lambda R^\sigma](R+m^*)\,. \tag{24}$$

The results of the calculation are not sensitive to which propagator is used.

4. BACKGROUND TERMS

These have been calculated in the papers of Le Bellac *et al.* and Vasavada. The deuteron pole graph (Fig. 2) occurs only in photodisintegration. We write the invariant coefficients:

$$H_i^{(1)}=4F\mu_d mR_i^{(1)}/(s-M^2)\,, \tag{25}$$

and then the only nonzero R_i are

$$R_1^{(1)}=mb\,,\quad R_5^{(1)}=a\,. \tag{26}$$

The nucleon exchange graphs (Fig. 3) contain the factor

$$1/D(t)=w(q^2)/(t-m^2)=1/(t-m^2)-1/(t-\beta'^2)\,, \tag{27}$$

where $\beta'^2=m^2+2(\beta^2-\alpha^2)$. Then we can write for the

[12] R. H. Dalitz and D. G. Sutherland, Phys. Rev. **146**, 1180 (1966).

[13] E. Ferrari and F. Selleri, Nuovo Cimento, Suppl. **24**, 453 (1962); Nuovo Cimento **27**, 1450 (1963).

[14] G. Mohan and S. C. Agarwal, Nuovo Cimento **37**, 431 (1964).

TABLE I. Invariant amplitudes.

i	I_i	ϵ_i
	(a) Photodisintegration	
1	$(1/2m^2)(\epsilon\cdot qk\cdot U-\epsilon\cdot Uq\cdot k)$	$+$
2	$(1/2m^2)(\epsilon\cdot Uk\cdot Q-\epsilon\cdot Qk\cdot U)$	$-$
3	$(1/m^4)(\epsilon\cdot qk\cdot Q-\epsilon\cdot Qq\cdot k)U\cdot q$	$-$
4	$(1/m^3)(\epsilon\cdot qk\cdot Q-\epsilon\cdot Qq\cdot k)\mathbf{U}$	$-$
5	$(1/2m)(\epsilon\cdot U\mathbf{k}-k\cdot U\gamma\cdot\epsilon)$	$+$
6	$(1/2m^3)((\epsilon\cdot Q\mathbf{k}-k\cdot Q\gamma\cdot\epsilon)U\cdot k-2(\epsilon\cdot q\mathbf{k}-q\cdot k\gamma\cdot\epsilon)U\cdot q)$	$+$
7	$(1/2m^3)((\epsilon\cdot q\mathbf{k}-q\cdot k\gamma\cdot\epsilon)U\cdot k+2(\epsilon\cdot Q\mathbf{k}-Q\cdot k\gamma\cdot\epsilon)U\cdot q)$	$-$
8	$(1/4m^2)[\gamma\cdot\epsilon,\mathbf{k}]U\cdot k$	$+$
9	$(1/2m^2)[\gamma\cdot\epsilon,\mathbf{k}]U\cdot q$	$-$
10	$(1/2m^2)\{[\mathbf{U},\gamma\cdot\epsilon]q\cdot k-[\mathbf{U},\mathbf{k}]\epsilon\cdot q+2\epsilon\cdot QU\cdot k-2\epsilon\cdot UQ\cdot k\}$	$-$
11	$(1/2m^2)\{[\mathbf{U},\gamma\cdot\epsilon]Q\cdot k-[\mathbf{U},\mathbf{k}]\epsilon\cdot Q+2\epsilon\cdot qU\cdot k-2\epsilon\cdot Uq\cdot k\}$	$+$
12	$(1/2m)i\gamma_5\epsilon^{\mu\nu\rho\sigma}\gamma_\rho k_\sigma\epsilon_\mu U_\nu$	$-$
	(b) Pionic disintegration	
1	$(1/2m)\gamma_5 U\cdot k$	$-$
2	$(1/m)\gamma_5 U\cdot q$	$+$
3	$\gamma_5\mathbf{U}$	$-$
4	$(1/2m)\gamma_5[\mathbf{k},\mathbf{U}]$	$+$
5	$(1/2m^2)\gamma_5 U\cdot k\mathbf{k}$	$-$
6	$(1/m^2)\gamma_5 U\cdot q\mathbf{k}$	$+$

isovector and isoscalar parts of H_i

$$H_i^{V(n)}=2mG_V^{(n)}R_i^{(n)}[1/D(t)-\epsilon_i/D(u)], \quad (28)$$

$$H_i^{S(n)}=2mG_S^{(n)}R_i^{(n)}[1/D(t)+\epsilon_i/D(u)], \quad (29)$$

where $G_S^{(n)}$ and $G_V^{(n)}$ are the scalar and vector coupling constants for process n. For the pionic disintegration $G_V^{(2)}=\sqrt{2}gF$ and $G_S^{(2)}=0$. Then we find the nonzero $R_i^{(2)}$ to be

$$R_i^{(2)}=-a\,,\ R_4^{(2)}=-\tfrac{1}{2}a\,,\ R_5^{(2)}=-\tfrac{1}{2}b\,,\ R_6^{(2)}=\tfrac{1}{2}b\,. \quad (30)$$

In the case of photodisintegration we treat the two types of $NN\gamma$ vertices separately. For Dirac coupling $G_V^{(3)}=G_S^{(3)}=eF$. Then for the nonzero $R_i^{(3)}$ we find

$$\begin{aligned}&R_1^{(3)}=mb\,, && R_2^{(3)}=mbq\cdot k/Q\cdot k\,, && R_3^{(3)}=-m^3b/Q\cdot k\,,\\ &R_4^{(3)}=am^2/Q\cdot k\,, && R_5^{(3)}=a\,, && R_8^{(3)}=-\tfrac{1}{2}mb\,,\\ &R_9^{(3)}=\tfrac{1}{2}mb\,, && R_{12}^{(3)}=-a\,. && \end{aligned} \quad (31)$$

It should be noticed that Le Bellac *et al.* give $R_2^{(3)}$ as $-mb$ but we disagree with this value.

The Pauli coupling has $G_S^{(4)}=m(\kappa_p+\kappa_n)F$ and $G_V^{(4)}=m(\kappa_p-\kappa_n)F$. For the $R_i^{(4)}$ we find

$$\begin{aligned}&R_2^{(4)}=-mb\,, && R_4^{(4)}=\tfrac{1}{2}mb\,, && R_5^{(4)}=a\,,\\ &R_6^{(4)}=\tfrac{1}{2}mb\,, && R_8^{(4)}=-\tfrac{1}{2}mb\,, && R_{10}^{(4)}=\tfrac{1}{2}(a-mb)\,,\\ &R_{11}^{(4)}=\tfrac{1}{2}a\,, && R_{12}^{(4)}=-a+q^2b/m\,. && \end{aligned} \quad (32)$$

5. RESONANT TERMS

A. Energy-Denominator Integral

In order to calculate the resonant terms (Fig. 4), we must make two simplifying assumptions. The first assumption is due to Austern. It is that the intermediate particles are at almost at rest. In terms of the momenta shown in the diagram,

$$|\mathbf{R}|\ll|\mathbf{k}|\,,\quad |\mathbf{q}_2|\ll|\mathbf{k}|\,. \quad (33)$$

This assumption is only made in the denominator; while in the numerator where we wish to keep everything covariant we make a slightly different assumption, i.e., that

$$q_1=q_2=\tfrac{1}{2}d\,. \quad (34)$$

It will be seen below that only values of $-(q_1-q_2)^2<(100\text{ MeV})^2$ contribute to the integral and so this is a reasonable assumption.

With these assumptions we have to evaluate

$$\frac{1}{D'}=i\int\frac{d^4V}{(2\pi)^4}\frac{w(V^2)F(q_3^2)}{(R^2-m^{*2})(q_1^2-m^2)(q_2^2-m^2)(q_3^2-\mu^2)}\,, \quad (35)$$

where $V\equiv\tfrac{1}{2}(q_1-q_2)$.

Details of the integral can be found in Appendix C. The result is

$$\frac{1}{D'}=\frac{1}{2\pi^2}\frac{\{A+B\mu^2/[2m(E-m)+(C+1)\mu^2]\}[\Lambda-\alpha\arctan(\Lambda/\alpha)]}{2m[(d_0+k^0-m)^2-m^{*2}][2m(E-m)+\mu^2]}\,. \quad (36)$$

B. Resonant Pion Disintegration

In this case we can write

$$H_i^{(5)}=\tfrac{4}{3}\sqrt{2}(g\lambda^2F/\mu^2)(2m/D')R_i^{(5)V}\,, \quad (37)$$

where $R_i^{(5)V}\equiv R_i^{(5)}(s,t,u)-\epsilon_iR_i^{(5)}(s,u,t)$. The factor $\tfrac{4}{3}$ comes from isospin considerations as explained in Vasavada. In order to find the $R_i^{(5)V}$ we have to split $N^{(5)}$ into invariants where

$$\begin{aligned}N^{(5)}=\bar{u}(p_1)(R-p_1)^\mu P_{\mu\nu}(R)k^\nu&\\ \times(\tfrac{1}{2}\mathbf{d}+m)\mathbf{U}(\tfrac{1}{2}\mathbf{d}-m)\gamma_5C\bar{u}^T(p_2)\,,& \quad (38)\end{aligned}$$

where

$$R=\tfrac{1}{2}d+k=\tfrac{1}{2}(p_1+p_2+k)\,.$$

After a considerable amount of algebra, we find the result shown in Table II(a).

C. Resonant Photodisintegration

The invariant coefficients can be written

$$H_i^{(6)}=-2(\sqrt{\tfrac{2}{3}})ge(C_3\lambda F/\mu^2)(2m/D')R_i^{(6)V}\,, \quad (39)$$

where, again,

$$R_i^{(6)V}\equiv R_i^{(6)}(s,t,u)-\epsilon_iR_i^{(6)}(s,u,t)\,.$$

In this case the numerator is

$$N^{(6)}=2m\bar{u}(p_1)(R-p_1)^\mu p_{\mu\nu}(R)f^{\nu\rho}\gamma_\rho(\tfrac{1}{2}\mathbf{d}-m)\,\mathbf{U}C\bar{u}^T(p_2)\,. \quad (40)$$

TABLE II. Invariant coefficients.

i	$R^{(5)V}$
(a) Invariant coefficients in resonant pionic disintegration	
1	0
2	$(2wm^4/3\eta^2)[y(1-y)-\eta(1+3\eta+2\eta^2)]$
3	$(m^4/6\eta^2)[2(2+\eta-\eta^2)y^2+(4+5\eta-3\eta^2)\sigma y-2\eta(1+\eta)\sigma]$
4	$(2wm^4/3\eta^2)[y(1-y)-\eta(1+3\eta+2\eta^2)]$
5	$(-m^4/12\eta^2)[16\eta(1+\eta)+4y(2+\eta^2)-(1-7\eta)\sigma\eta-8y^2-8\sigma y]$
6	$(-wm^4/3\eta^2)[2y+\eta(1-5\eta)]$
(b) Invariant coefficients in resonant photodisintegration	
1	$(8m^4w/3\eta^2)(1+3\eta^2)$
2	$(-4m^4/3\eta^2)(2+\eta+3\eta^2+4\eta^3)-(4m^4y/3\eta^2)(3+4\eta+6\eta^2)$
3	$-8m^4$
4	$(2m^4/3\eta^2)(2+\eta+3\eta^2+4\eta^3)+(2m^4y/3\eta^2)(3+4\eta)$
5	$(-m^4w/3\eta)(1+3\eta+2\eta^2)+(2m^4yw/3\eta^2)(1-2\eta)$
6	0
7	$(2m^4/3\eta^2)(2-\eta-3\eta^2)+(2m^4y/\eta^2)$
8	$(2m^4w/3\eta^2)(2+\eta-11\eta^2+10y)$
9	$(2m^4/3\eta^2)(2+\eta-5\eta^2-4\eta^3)+(2m^4y/3\eta^2)(11-\eta-9\eta^2)$
10	$(2m^4/3\eta^2)(2+3\eta-\eta^2-8\eta^3)+(2m^4y/3\eta^2)(7+4\eta-6\eta^2+6\eta^3)$
11	$(-2m^4w/3\eta^2)(2+2\eta+2\eta^2-3y^2)$
12	$(2m^4/3\eta^2)(5-7\eta-21\eta^2-9\eta^3-9\eta y^2)+(5y^2m^4/\eta^2)$

The algebra in this case is so prohibitive that a computer was programmed to perform it, as explained in the Introduction. In the program, the p_1 and p_2 were eliminated and then each term in the sum is of the form

$$X^{\mu\nu\lambda}f_{\mu\nu}U_\lambda \quad \text{or} \quad X^{\mu\nu\lambda}f_{\mu\nu}U_\lambda \mathbf{k}\,, \tag{41}$$

where $X^{\mu\nu\lambda}$ is a tensor made up out of linear products of $p_{1\mu}$, $p_{2\mu}$, $g_{\mu\nu}$, and γ_μ. Each possible $X^{\mu\nu\lambda}$ not eliminated by symmetry, must then be expanded in terms of the invariants. The result is shown in Table II(b).

6. COMPARISON WITH EXPERIMENT

A. Background

It will be seen from Figs. 6 and 7 that it is impossible to achieve agreement with experiment for a value of ρ greater than 0.6%. There are a number of possible explanations.

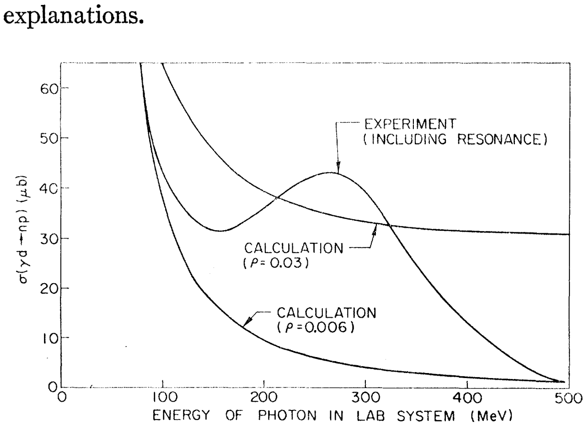

FIG. 6. The calculated background cross section compared with the experimental results for the total (i.e., including resonance) cross section for photodisintegration.

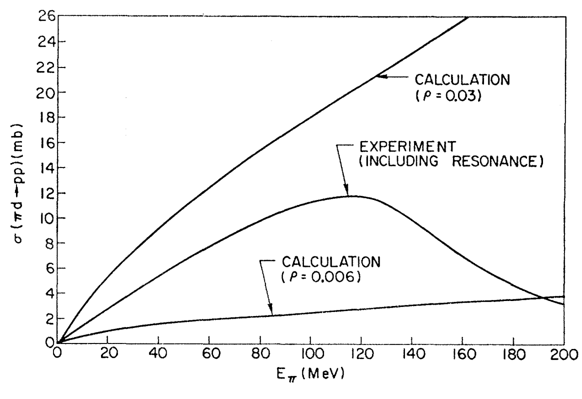

FIG. 7. Same as for Fig. 6 but for pionic disintegration.

First, the Hulthén wave function cannot be correct for the D state of the deuteron because it has the wrong behavior in real space in the vicinity of the origin. However, it is doubtful that it could be so incorrect as to produce such a large discrepancy. If a different D-state wave function is assumed which does have the correct behavior, as was done by Le Bellac *et al.*, three extra parameters are introduced. With the choices made by Le Bellac *et al.*, it is still not possible to obtain a good fit in the high-energy region.

Secondly, when we wrote down the dNN vertex, we neglected terms which vanish in the limit $q^2+\alpha^2 \to 0$. These terms are not negligible, as they are in the low- and intermediate-energy ranges, but we have no way of calculating them.

Finally, it is possible that final-state corrections are to blame. This is unlikely as the phase shifts for pp elastic scattering, which would be used for a distorted-wave Born calculation, are relatively small. No amount of final-state correction could produce the 80% reduction of background necessary to obtain a good fit with experiment.

Lacking ways to overcome these three faults, we use a phenomenological adjustment of the D-state admixture parameter ρ. It is gratifying that the same value of ρ can be used to fit both types of disintegration.

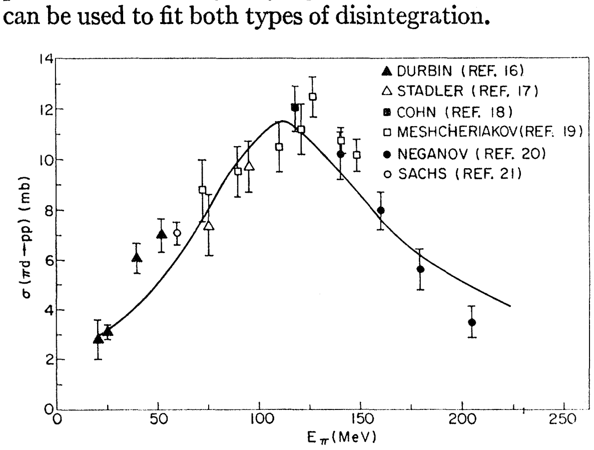

FIG. 8. The pionic disintegration total cross section as a function of the energy of the pion in the c.m. system.

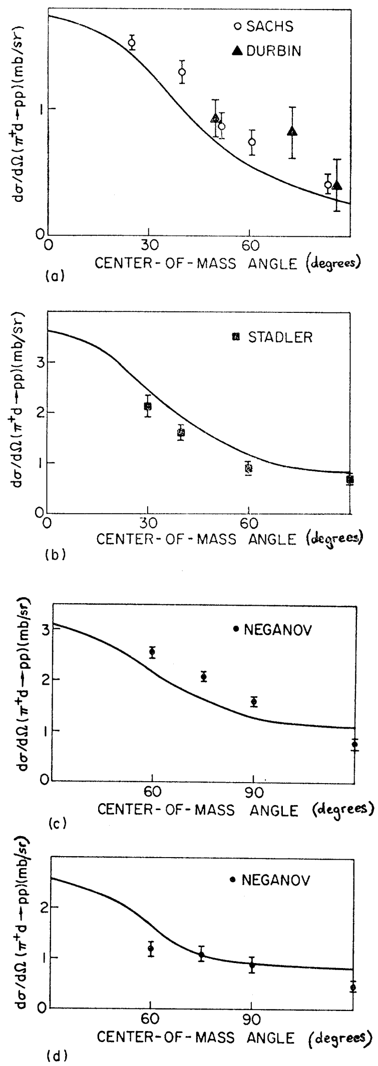

FIG. 9. The pionic disintegration differential cross section as a function of angle at various energies: (a) $E_\pi=40$ MeV; (b) $E_\pi=76$ MeV; (c) $E_\pi=140$ MeV; (d) $E_\pi=180$ MeV.

B. Total Calculation

In order to achieve peaking at the correct energy we have to use a resonant mass of 1190 MeV instead of 1236 MeV as indicated by photoproduction. The reason for this is not known but has been noticed by other authors.

The cutoff Λ is taken as $2.60\,\alpha$ which is close to the value $2.53\,\alpha$ used by Barshay.[15] Then the results are presented in Figs. 8–14. (See Refs. 16–31.)

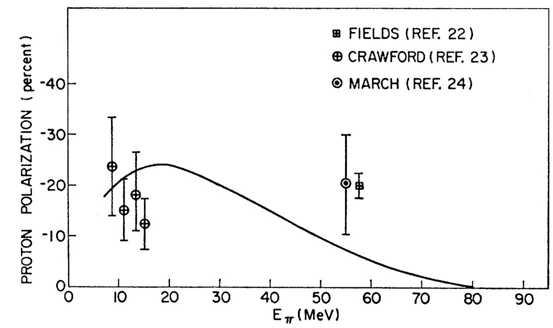

FIG. 10. The proton polarization at 90° in pionic disintegration as a function of energy.

The pionic disintegration total cross section and differential cross section are well fitted up to about 180 MeV. This energy marks the approximate threshold for two-pion production which is the probable explanation for the failure of the theory in this region.

The polarization points in Fig. 10 are taken from the inverse reaction, $pp\rightarrow\pi^+d$ and are fairly well fitted.

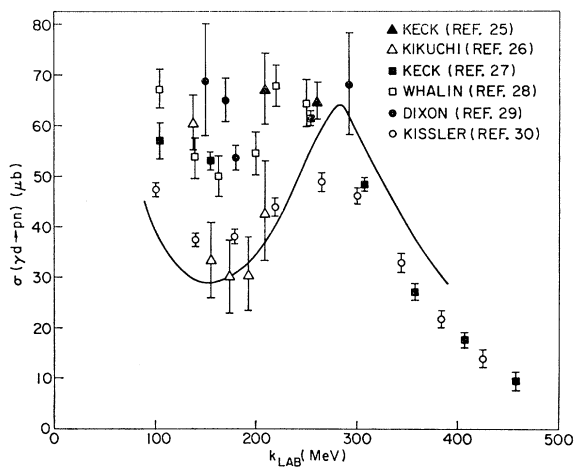

FIG. 11. The photodisintegration total cross section as a function of the energy of the photon in the laboratory.

[15] S. Barshay, Phys. Rev. Letters **17**, 49 (1966).
[16] R. Durbin, H. Loar, and J. Steinberger, Phys. Rev. **84**, 581 (1951).
[17] H. L. Stadler, Phys. Rev. **96**, 496 (1954).
[18] C. E. Cohn, Phys. Rev. **105**, 1582 (1957).
[19] M. G. Meshcheriakov and B. S. Neganov, Dokl. Akad Nauk SSSR **100**, 617 (1955).
[20] B. S. Neganov and L. B. Parfenov, Zh. Eksperim. i Teor. Phys. **34**, 767 (1958) [English transl.: Soviet Phys.—JETP **7**, 528 (1958)].
[21] A. M. Sachs, H. Winick and B. A. Wooten, Phys. Rev. **109**, 1733 (1958).
[22] T. H. Fields, J. G. Fox, J. A. Kane, R. A. Stallwood, and R. B. Sutton, Phys. Rev. **95**, 638 (1954); **109**, 1704 (1958).
[23] F. S. Crawford and M. L. Stevenson, Phys. Rev. **97**, 1305 (1955).
[24] R. H. March, Phys. Rev. **120**, 1874 (1960).
[25] J. Keck, R. M. Littauer, G. K. O'Neill, A. M. Perry, and W. M. Woodward, Phys. Rev. **93**, 827 (1954).
[26] S. Kikuchi, Phys. Rev. **85**, 1062 (1952).
[27] J. C. Keck and A. V. Tollestrup, Phys. Rev. **101**, 360 (1956).
[28] E. A. Whalin, B. D. Schriever, and A. O. Hanson, Phys. Rev. **101**, 377 (1956).
[29] D. R. Dixon and K. C. Pandtel, Phys. Rev. **104**, 1730 (1956).
[30] K. H. Kissler, R. Kose, W. Paul, and K. Stockhorst, in Proceedings of the International Symposium on Electron and Photon Interactions at High Energy, Hamburg 1965 (unpublished).
[31] G. Barbiellini, C. Bernadini, F. Felicetti, G. P. Murtas, and Frascali, in Proceedings of the International Conference on Low and Intermediate Energy Electromagnetic Interactions, Dubna (USSR), 1967 (unpublished).

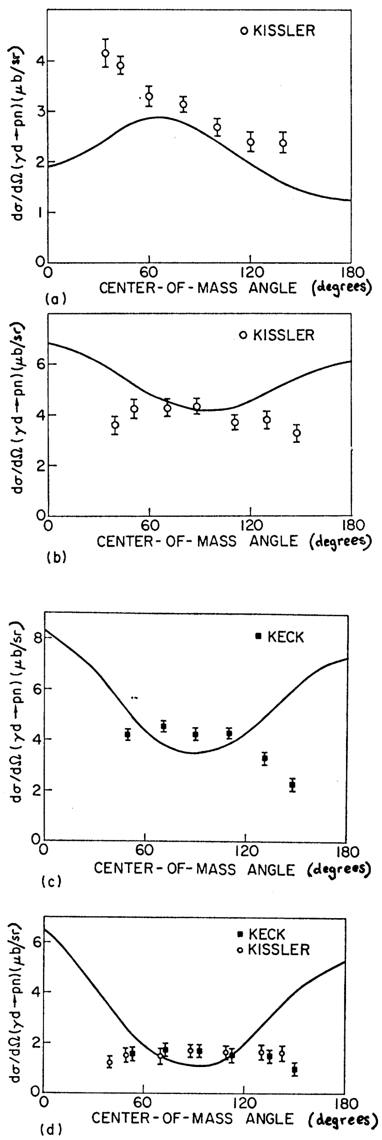

FIG. 12. The photodisintegration differential cross section as a function of angle at various energies: (a) $k_L=40$ MeV; (b) $k_L=260$ MeV; (c) $k_L=300$ MeV; (d) $k_L=390$ MeV.

With the values of m^*, ρ, and Λ taken from pionic disintegration we plotted the photodisintegration results of Figs. 11–14. The differential cross section is predicted to have large forward and backward scattering, a fact which is not borne out by experiment. Any mechanism reducing the forward and backward cross sections would presumably also appear in pionic disintegration but cannot be seen there. This is the most puzzling result of the calculation.

The real success of this work is in correctly predicting the asymmetry at high energies (Fig. 13). Although there is some disagreement at 90° in the c.m. system at low-energies, we get good results elsewhere.

In the proton polarization we get qualitative agreement (Fig. 14) though again there is failure at the highest energy.

The reason that the polarization results are better than the asymmetry results probably lies in our approximation of the integral in Eq. (35). The polarization is independent of the value of this integral so long as the resonance dominates. All the helicity amplitudes are

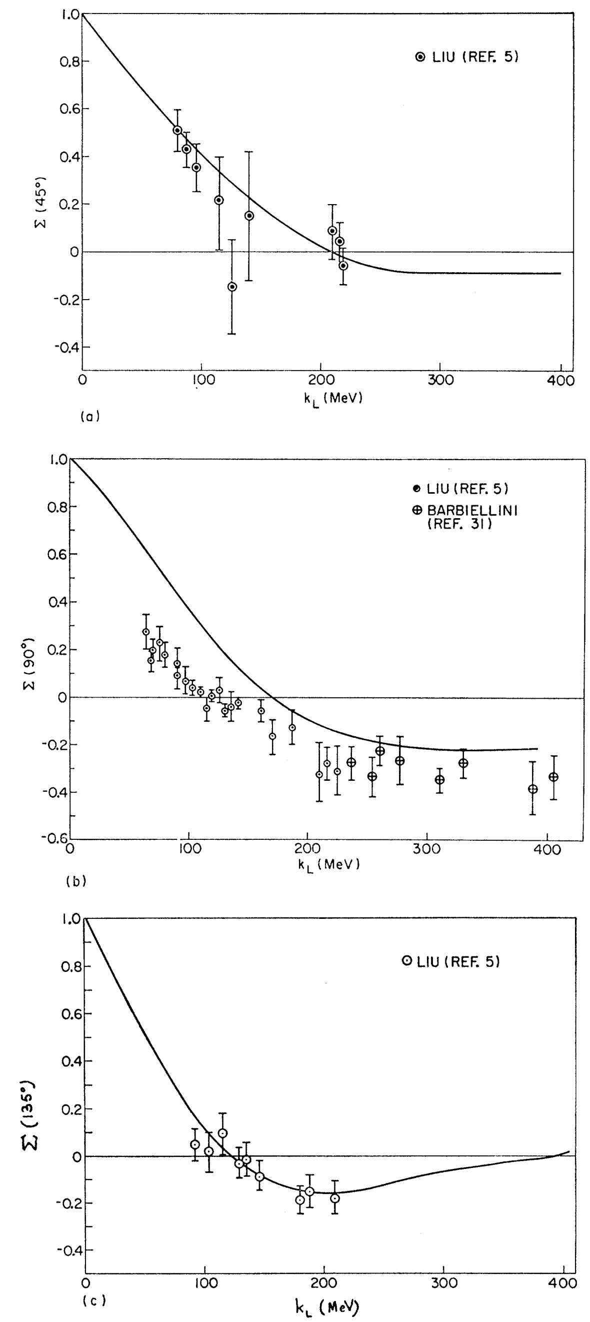

FIG. 13. The asymmetry in photodisintegration as a function of energy at various c.m. angles: (a) $\theta_{c.m.}=45°$; (b) $\theta_{c.m.}=90°$; (c) $\theta_{c.m.}=135°$.

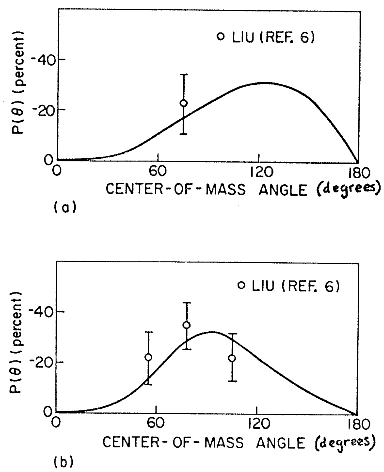

FIG. 14. The proton polarization in photodisintegration as a function of angle at various energies: (a) $k_L=200$ MeV; (b) $k_L=350$ MeV.

multiplied by it and so it cancels from Eqs. (9), (11), and (12). The differential cross section, on the other hand, depends very much on the approximation to the integral.

In summary, the main advantages and disadvantages of the Austern model are maintained in a relativistic formulation. It does not correctly predict the shape of the photodisintegration cross section but otherwise it is in excellent agreement with experiment, including the new measurements of asymmetry and polarization.

ACKNOWLEDGMENTS

We wish to thank Professor A. C. Hearn for his help and guidance in the course of this work.

APPENDIX A

We shall use the metric $g_{00}=-g_{11}=-g_{22}=-g_{33}=1$ so that

$$A^{\mu}B_{\mu}=A\cdot B=A^0B^0-\mathbf{A}\cdot\mathbf{B}. \qquad \text{(A1)}$$

The Dirac equation is

$$\not{p}u=mu. \qquad \text{(A2)}$$

The spin matrices are $\sigma^{\mu\nu}=\frac{1}{2}i[\gamma^{\mu},\gamma^{\nu}]$ and $\gamma_5=i\gamma_0\gamma_1\gamma_2\gamma_3$. A useful formula in our notation is

$$i\gamma_5\epsilon_{\mu\nu\lambda\sigma}\gamma^{\lambda}R^{\sigma}=\gamma_{\mu}\gamma_{\nu}\not{R}+R_{\mu}\gamma_{\nu}-R_{\nu}\gamma_{\mu}-g_{\mu\nu}\not{R}. \qquad \text{(A3)}$$

APPENDIX B

The helicity amplitudes are defined in pionic disintegration by

$$\begin{aligned} F_{1\pm}&=\langle 1|T|\pm\tfrac{1}{2}\pm\tfrac{1}{2}\rangle,\\ F_{2\pm}&=\langle -1|T|\pm\tfrac{1}{2}\mp\tfrac{1}{2}\rangle,\\ F_{3\pm}&=\langle 0|T|\tfrac{1}{2}\pm\tfrac{1}{2}\rangle, \end{aligned} \qquad \text{(B1)}$$

where we have written $\langle\lambda_D|T|\lambda_N,\lambda_N'\rangle$ for the T-matrix element. It is straightforward to show that

$$\begin{aligned} F_{1\pm}&=\mp(\sin\theta/\sqrt{2}m^2)[Ep H_2\mp(Ek\pm k^0p)H_4-pk^0H_6],\\ F_{2\pm}&=[(1\mp z)/\sqrt{2}m^2][\pm pH_3+kH_4\\ &\qquad-(p^2k/m^2)(1\pm z)H_6],\\ F_{3+}&=(1/m^2M)[E^2kH_1+d^0EpzH_2-mkH_3\\ &\qquad+(\mu^2-2Ek^0)pzH_4-Ekk^0H_5-k^0pzH_6],\\ F_{3-}&=(\sin\theta/Mm)[pd^0H_3-(pEk^2/m^2)H_5\\ &\qquad-(p^2kd^0z/m^2)H_6]. \end{aligned} \qquad \text{(B2)}$$

The helicity amplitudes for photodisintegration are the same as those of Le Bellac *et al.*,[8] and their relationship to the H_i can also be found in that paper.

APPENDIX C

We wish to calculate the integral

$$\frac{1}{D'}=i\int\frac{d^4V}{(2\pi)^4}\frac{w(V^2)F(q_3^2)}{(R^2-m^{*2})(q_1^2-m^2)(q_2^2-m^2)(q_3^2-\mu^2)}. \qquad \text{(C1)}$$

The dV^0 integral can be approximated by the residue from the pole of $q_2^2-m^2$, which is easily shown to occur at

$$V_{\pm}^0=\tfrac{1}{2}d^0\pm m[1+(1/2m^2)(\mathbf{V}+\tfrac{1}{2}\mathbf{k})^2-i\epsilon], \qquad \text{(C2)}$$

where ϵ is the small, positive imaginary part of the nucleon mass. Then we see

$$\frac{1}{D'}=\int\frac{d^3V}{(2\pi)^3}\frac{w(V^2)F(q_3^2)}{2m(q_1^2-m^2)(R^2-m^{*2})(q_3^2-\mu^2)}, \qquad \text{(C3)}$$

where everything is evaluated at $V^0=V_-^0$.

Upon evaluation we find

$$\begin{aligned} q_1^2-m^2&\approx-2(\mathbf{V}^2+\alpha^2),\\ R^2&\approx(d^0+k^0-m)^2,\\ q_3^2&\approx 2m(m-E), \end{aligned} \qquad \text{(C4)}$$

so that (C3) becomes

$$\frac{1}{D'}=\frac{1}{2m[(d^0+k^0-m)^2-m^{*2}][2m(E-m)+\mu^2]}\times\left\{A+\frac{B\mu^2}{2m(E-m)+(C+1)\mu^2}\right\}\int\frac{d^3V}{(2\pi)^3}\frac{w(V^2)}{\mathbf{V}^2+\alpha^2}. \qquad \text{(C5)}$$

The integral in (C5) does not converge and so we introduce a cutoff Λ:

$$\int\frac{d^3V}{(2\pi)^3}\frac{w(\mathbf{V}^2)}{\mathbf{V}^2+\alpha^2}\rightarrow 4\pi\int_0^{\Lambda}\frac{V^2dVw(V^2)}{V^2+\alpha^2}=4\pi[\Lambda-\alpha\arctan(\Lambda/\alpha)+O(\Lambda^3/\beta^2)]. \qquad \text{(C6)}$$

We can ignore $O(\Lambda^3/\beta^2)$ which merely amounts to a small shift in the cutoff. As the cutoff has no physical significance, this is justified.